

See discussions, stats, and author profiles for this publication at: <https://www.researchgate.net/publication/2318927>

# An Algorithm for Synaptic Modification Based on Exact Timing of Pre- and Post-Synaptic Action Potentials

Article · February 1999

Source: CiteSeer

CITATIONS

8

READS

25

2 authors:



Walter Senn

Universität Bern

158 PUBLICATIONS 4,752 CITATIONS

[SEE PROFILE](#)



Michail Tsodyks

Columbia University

200 PUBLICATIONS 13,721 CITATIONS

[SEE PROFILE](#)

Some of the authors of this publication are also working on these related projects:



Braintool [View project](#)



Human Brain Project [View project](#)

# An algorithm for synaptic modification based on exact timing of pre- and post-synaptic action potentials

Walter Senn<sup>1,2</sup>, Misha Tsodyks<sup>2</sup> and Henry Markram<sup>2</sup>

<sup>1</sup> Physiologisches Inst., Universität Bern, Bülhplatz 5, 3012 Bern, Switzerland

<sup>2</sup> Dept. of Neurobiology, The Weizmann Institute, Rehovot, 76100, Israel

**Abstract.** The timing between individual pre- and post-synaptic action potentials is known to play a crucial role in the modification of the synaptic efficacy during activity. Based on stimulation protocols of two synaptically connected neurons, we infer an algorithm which explains the data by modifying the probability of neurotransmitter discharge as a function of the pre- and postsynaptic spike delays. The characteristics of this algorithm is its asymmetry with respect to the delays: if the postsynaptic spike arrives *after* the presynaptic spike, the probability of discharge is up-regulated while it is down-regulated if the postsynaptic spike arrives *before* the presynaptic spike. The algorithm allows to predict stimulation protocols which induce maximal up- and down-regulation of the discharge probability.

## 1 Introduction

Since the work of D. Hebb [1], several attempts were made to formulate precise 'learning rules', which determine the change in synaptic efficacies from the known activities of neurons [2, 3, 4]. In these rules neuronal activities are represented by an analog variable reflecting the average firing rates of the neurons. Such formulations were used in training neural networks to perform various computational tasks.

Recent experimental developments indicate that a novel approach to modeling synaptic plasticity is needed. In [5], it was found that synaptic modification is very sensitive to the relative timing between the spike trains. If postsynaptic spikes occur 10ms after the presynaptic one, synaptic responses were increased. The same pattern of stimulation with the opposite time delay resulted in a decrease of responses. In [6] it was shown that the synaptic modification is a complex *redistribution* of synaptic efficacy between the spikes in the train without uniform strengthening of the connections. This redistribution can result from the increase in the probability of neurotransmitter release [7].

Experiments of [5] for the first time provide the experimental basis for formulating the learning rules based on individual spikes rather than firing rates. In the current contribution, we present what we believe is the minimal phenomenological model which reproduces the experimental results and which allows the computation of the synaptic modification for arbitrary patterns of spikes. This

model can now be tested against other experimental paradigms and provides a useful foundation for computational models which utilize exact spike timing for information processing [8].

## 2 The algorithm

The learning rule enables adaptation of the probability of neurotransmitter release resulting from simultaneous activity of pre- and post-synaptic neurons. Specifically, we adapt the probability that a presynaptic spike discharges a vesicle which is ready at the site of release. We refer to this probability as the probability of discharge,  $P_{dis}$ . The biophysical processes involved in modifying  $P_{dis}$  are triggered either by pre- or post-synaptic spikes, by a spontaneous presynaptic release or by elevation of the postsynaptic membrane potential. We assume that the up-regulation of  $P_{dis}$  is only induced by a postsynaptic spike following a presynaptic release. Down-regulation of  $P_{dis}$ , on the other hand, is only induced by a presynaptic release following a postsynaptic spike or voltage increase.

Practically, long-lasting synaptic modification does not instantaneously follow the pairing but develops slowly to peak within  $\approx 20$ min. Accordingly,  $P_{dis}$  is kept fixed during the simulated pairing and effects of each spike are summed up to determine the overall change in the *limit* probability  $P_{dis}^\infty$  (Fig. 1). The convergence of  $P_{dis}$  to the limit probability  $P_{dis}^\infty$  evolves with time constant  $\tau_{mod}^P = 20$ min. This work does not include a short lasting up-regulation of  $P_{dis}$  analogous to post tetanic potentiation because this phenomenon is not clearly evident at these depressing synapses. Neither considered is the decay of any change in  $P_{dis}$  (i.e. natural decay of  $P_{dis}^\infty$ ) which could occur on a time scale of hours.

In detail, the synaptic modification works as follows. The primary events for up- and down-regulation are mediated by the NMDA-receptors located at the postsynaptic membrane. These receptors may be in 3 different states: the recovered state,  $N_{rec}$ , the state saturated with glutamate,  $N_u$ , and the state altered by intracellular calcium,  $N_d$  (Fig. 1). The secondary messenger for up- and down-regulation may be in an active state,  $S_u$  and  $S_d$ , or in an inactive state,  $\bar{S}_u$  and  $\bar{S}_d$ , respectively. If a vesicle of neurotransmitter discharges, either spontaneously or due to a presynaptic spike, glutamate is released and bound by postsynaptic NMDA-receptors ( $N_{rec} \rightarrow N_u$ ). Being in a state saturated by glutamate, the NMDA-receptors will open when a back-propagating postsynaptic spike arrives or, more generally, when the postsynaptic membrane potential increases allowing calcium to flow through NMDA-channels into the postsynaptic cell. This calcium activates a secondary messenger ( $\bar{S}_u \rightarrow S_u$ ) which diffuses to the presynaptic site and up-regulates the probability of discharge ( $\bar{P}_{dis}^\infty \rightarrow P_{dis}^\infty$ ). If, on the other hand, there is first an increase of the postsynaptic membrane potential e.g. due to a postsynaptic spike, voltage activated calcium-channels open, calcium flows in through these channels and binds to the NMDA-receptors [9], altering or redirecting their function ( $N_{rec} \rightarrow N_d$ ). Subsequently released glutamate now activates an altered NMDA receptor which

leads to the activation of down-regulating secondary messenger ( $\bar{S}_d \rightarrow S_d$ ). This messenger diffuses to the presynaptic location and the probability of discharge is down-regulated ( $P_{dis}^\infty \rightarrow \bar{P}_{dis}^\infty$ ).

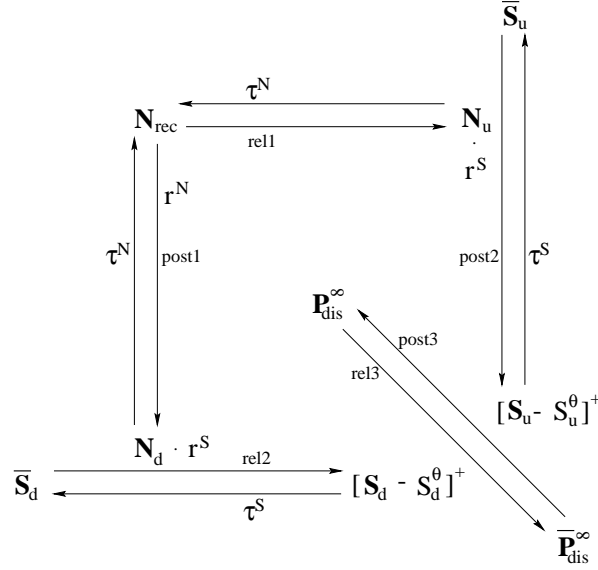


**Fig. 1.** The kinetic scheme for modification of the limit probability of discharge,  $P_{dis}^\infty$ . Up-regulation of  $P_{dis}^\infty$  is mediated through the states  $N_u$  and  $S_u$  while down-regulation is mediated through the states  $N_d$  and  $S_d$ . These states decay naturally with time constants  $\tau^N$  and  $\tau^S$ , respectively. Transitions labeled with *rel*<sub>*i*</sub> and *post*<sub>*i*</sub> (*i*=1,2,3) occur instantaneously at either a presynaptic release or at a postsynaptic spike. These instantaneous transitions are weighted by the factors written onto their arrows. For instance, at a postsynaptic spike, the state  $N_d$  is increased by  $N_{rec} \cdot r^N$  (*post1*) and the state  $S_u$  is increased by  $\bar{S}_u \cdot N_u \cdot r^S$  (*post2*). At a presynaptic release, for instance,  $P_{dis}^\infty$  is decreased by  $P_{dis}^\infty \cdot [S_d - S_d^\theta]^+$  (*rel3*).

The above scenario can be summarized in the following 'learning algorithm'. Whenever a postsynaptic action potential arrives at the synaptic site, 3 different processes are induced (indicated by *post1* - *post3* in the scheme):

- post1* The fraction  $r^N$  of  $N_{rec}$  is moved to  $N_d$ . This describes the altering of NMDA-receptors due to calcium flowing into the postsynaptic site through voltage activated channels.
- post2* The fraction  $r^S N_u$  of  $\bar{S}_u$  is moved to  $S_u$  ( $\bar{S}_u = 1 - S_u$ ). This describes the activation of up-regulating secondary messenger proportional to the amount of NMDA-receptors saturated with glutamate.
- post3* The limit probability  $P_{dis}^\infty$  is increased by  $\bar{P}_{dis}^\infty [S_u - S_u^\theta]^+$ , where  $\bar{P}_{dis}^\infty = 1 - P_{dis}^\infty$  and  $S_u^\theta$  denotes the threshold to trigger up-regulation ( $[x]^+ =$

$\max(x, 0)$ ). Thus,  $P_{dis}^\infty$  is pushed towards 1 proportional to the amount of secondary messenger above threshold.

A release of a vesicle at the presynaptic site induces, completely symmetrically, the following 3 processes (indicated by *rel1* - *rel3* in the scheme):

- rel1 The available amount of  $N_{rec}$  is moved to  $N_u$ . This describes the saturation of the recovered NMDA-receptors with glutamate.
- rel2 The fraction  $r^S N_d$  of  $\tilde{S}_d$  is moved to  $S_d$  ( $\tilde{S}_d = 1 - S_d$ ). This describes the activation of down-regulating secondary messenger proportional to the amount of altered NMDA-receptors.
- rel3 The limit discharge probability is reduced by  $P_{dis}^\infty [S_d - S_d^\theta]^+$ , i.e. proportional to  $P_{dis}^\infty$  and to the amount of  $S_d$  above threshold  $S_d^\theta$ .

In a temporal order, up- and down-regulation of  $P_{dis}^\infty$  are each mediated by a primary and secondary event (cf. scheme): The primary event for up-regulation is a presynaptic release (*rel1*) and the secondary event is a postsynaptic spike (*post2*). The primary event for down-regulation is a postsynaptic spike (*post1*) and the secondary event is a presynaptic release (*rel2*). Beside these instantaneous transitions, the states  $N_u$ ,  $N_d$  and  $S_u$ ,  $S_d$  decay exponentially with the corresponding time constants  $\tau^N$  and  $\tau^S$ , respectively.

To describe the synaptic depression we implemented a vesicle depletion model according to which a vesicle recovers stochastically after a release with time constant  $\tau_{rec}^P = 800\text{ms}$ . Due to this recovery process, a spike following shortly after a previous discharge has less chance to encounter an occupied site of release and thus less chance to discharge a vesicle. Averaging over an ensemble of synapses, the model turns into the deterministic model of a depressing synapse [7] and  $P_{dis}$  represents the *use of synaptic efficacy* ( $U_{SE}$ ).

### 3 Application of specific stimulation protocols

The algorithm is based on dual whole-cell voltage recordings of neocortical pyramidal cells [5]. It was tested against the following 3 experiments:

Experiment1: Pre- and postsynaptic spike trains of 10Hz and 5 spikes were paired with a time difference between post- and presynaptic spikes of +10 and -10ms, respectively. The pairing was repeated 10 times every 4s and the change in  $P_{dis}$  was recorded for the next 60min. The increase in  $P_{dis}^\infty$  for the 10ms retarded postsynaptic spikes and the decrease for the 10ms advanced postsynaptic spikes was faithfully reproduced by the algorithm (simulation results Fig. 2a, experimental data [5, Fig. 3C]).

Experiment2: Paired pre- and postsynaptic spikes trains of 5 spikes were triggered with a postsynaptic delay of 2ms. The simulation was performed for different frequencies ranging from 2 to 40Hz and the final change in the probability of discharge,  $P_{dis}^\infty$ , is evaluated. The main characteristics of the learning curve, the steep upstroke at 10Hz and the saturation at higher frequencies, are well reproduced (simulation results Fig. 3a, experimental data [5, Fig. 2C]).

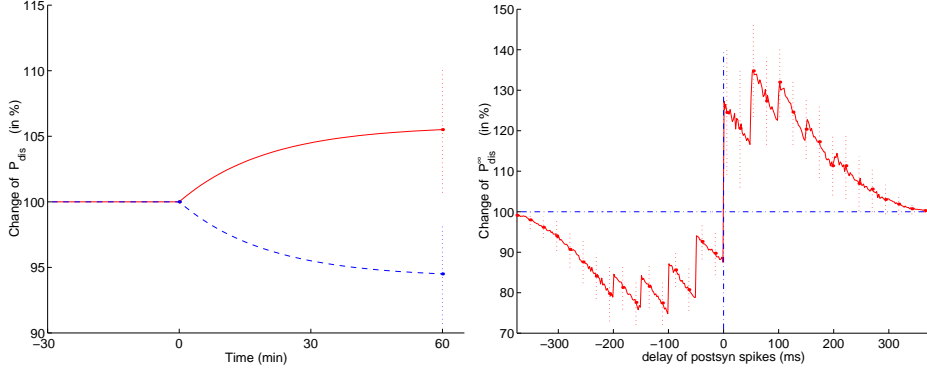


**Fig. 2.** Modification of  $P_{dis}$  as a function of the postsynaptic spike delays. **a** *Exp1:* The evolution of  $P_{dis}$  towards  $P_{dis}^{\infty}$  induced by repeated pairings at 10Hz with delay of 10ms (upper trace) and  $-10ms$  (lower trace). The parameters in all our simulations are  $r^N = .5$ ,  $\tau^N = 300ms$ ,  $r^S = .7$ ,  $\tau^S = 600ms$ . The thresholds for the secondary messengers were set to  $S_u^{\theta} = r^S$  and  $S_d^{\theta} = r^N r^S$ . As starting values for the discharge probabilities we chose  $P_{dis} = P_{dis}^{\infty} = .5$ . **b** A prediction: Change of  $P_{dis}$  after pairing of 20Hz trains of 5 spikes with delays ranging from  $-350$  to  $350ms$ . Pointed lines represent standard deviations.

Experiment3: Pre- and post-synaptic spike trains of 20Hz were paired with a postsynaptic spike delay of 2ms. The number of spikes in the paired trains were varied from 2 up to 20 and for each number  $P_{dis}^{\infty}$  was determined. The astonishing fact in this experiment was that the change in  $P_{dis}^{\infty}$  did not accumulate but was rather neutralized by the following spikes (Markram, unpublished). Simulations of the model are compatible with these results (Fig. 3b).

Apart from reproducing existing experiments, the algorithm produces hypotheses about the outcome of new experiments. One of the remaining questions is the change in  $P_{dis}$  for pre- and postsynaptic spike trains of a given frequency and varying delays. Figure 2b shows the relative change in  $P_{dis}^{\infty}$  for spike trains of 5 spikes at 20Hz with different delays of the postsynaptic train. Notice that down-regulation is maximal at a presynaptic delay of 100ms while up-regulation is maximal at a postsynaptic delay of 50ms. The delay of  $-100ms$  is explained by the fact that at a postsynaptic spike only the fraction  $r^N$  of  $N_{rec}$  is moved to  $N_d$  and the delay of 50ms is explained by the fact that not each presynaptic spike induces a neurotransmitter release.

## 4 Conclusion

The presented algorithm predicts the change in a specific synaptic property as a result of coherent activity of neurons and reproduces experimental observations of [5]. It confirmed three characteristics of the synaptic modification: 1. the asymmetry with respect to delays, 2. the monotonic increase with respect to the

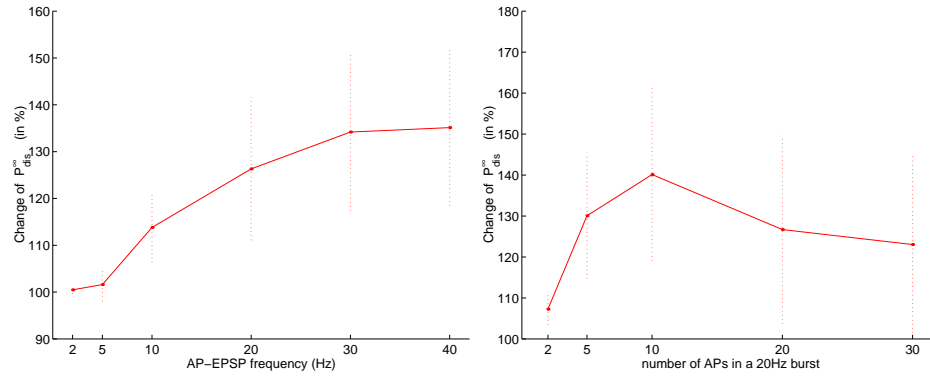


**Fig. 3.** The change in  $P_{dis}$  shown 60 minutes after pairing. **a** Exp2: Dependence on the frequency of the paired spike trains, each composed of 5 spikes. **b** Exp3: Dependence on the number of spikes within the paired 20Hz spike trains.

common pre- and postsynaptic frequency above 5Hz and 3. the non-monotonic dependence of the number of spikes in the paired trains. In agreement with [6], the algorithm does not predict the uniform increase of the synaptic strength.

One could speculate that due to additional computation such as the integration of a third coincident signal provided by growth factors or neuromodulators (e.g. synaptic growth or unmasking of postsynaptic receptors [10]) is required for the induction of real synaptic strengthening. Specifying these conditions remains an important challenge for a future research.

**Acknowledgment** We thank Josef Kleinle for critically reading the manuscript. This study was supported by an ONR grant and a SNF grant (5002-037939) for WS.

## References

1. Hebb, D.O. *The organization of behavior*, J. Wiley and Sons, New York (1949)
2. Bienenstock, E.L. & Cooper, L.N. & Munro, P.W. *J. Neuroscience* **2**(1), 32-48 (1982)
3. Sejnowski, T. *J. Math. Biol.* **4**, 303-321 (1977)
4. Artola, A. & Singer, W. *TINS* **16**(11), 480-487 (1993)
5. Markram, H. & Lübke, J & Forster, M & Sakmann, B. *Science* **275**, 213-215 (1997)
6. Markram, H. & Tsodyks, M. *Nature* **382**, 807-810 (1996)
7. Tsodyks, M. & Markram, H. *Proc. Natl. Acad. Sci. USA* **94**, 719-723 (1997)
8. Hopfield, J.J. *Nature* **376**, 33-36 (1995)
9. Mayer, M.L. & McDermott, A.B. & Westbrook, G.L. & Smith, S.J. & Barker, J.L. *J. Neuroscience* **7**, 3230-3244 (1987)
10. Liao, D. Z. & Hessler, N. A. & Malinow, R. *Nature* **375**, 400-404 (1995).